ELSEVIER

Polymer 42 (2001) 9827–9835

polymer

www.elsevier.com/locate/polymer

# Flow birefringence and strain-induced hardening of cycloolefin copolymers under elongational flow

Pralay Maiti, Masami Okamoto*, Tadao Kotaka

*Advanced Polymeric Materials Engineering, Graduate School of Engineering, Toyota Technological Institute, Hisakata 2-12-1, Tempaku, Nagoya 468-8511, Japan*

Received 15 February 2001; received in revised form 14 June 2001; accepted 2 July 2001

**Abstract**

Strain-induced hardening behavior and flow birefringence were studied on copolymers of ethylene–tetracyclododecene (E–TD) and ethylene–norbornene (E–NB) of various compositions subjected to uniaxial elongation with constant Hencky strain rate between 0.01 and 1.0 $s^{-1}$ in the temperature range from +40 to +60°C above their respective glass transition $T_g$. When compared at the corresponding temperature of, e.g. $T_g$ + 50°C, the E–TD copolymer exhibited stronger tendency of strain-induced hardening than the E–NB copolymer of the corresponding comonomer content. The stress optical rule (SOR) was obeyed for the E–NB copolymer in the whole range of its composition, while for the E–TD copolymer, the SOR was valid only for that of low TD content (<30 mol%), but invalid for that of high TD (≥30 mol%) content. The results suggest that the increase in the population of bulkier TD comonomer may be a molecular origin of the strong strain-induced hardening as well as a reason for the invalidity of SOR for the E–TD copolymer of high TD content. For the two copolymers that satisfy SOR, the stress optical coefficient $C$ decreases exponentially with the comonomer content, and the tendency is stronger for E–TD than for E–NB, reflecting the comonomer size. The stress optical coefficient $C$ vs. composition plots of the E–NB (block type) and E–TD copolymers are extrapolated at zero E limit to $5.5 \times 10^{-10}$ and $7.5 \times 10^{-12}$ $Pa^{-1}$, respectively, which are expected to be the $C$ for the NB and TD homopolymers if such polymers do exist. 

*Keywords*: Elongational flow; Strain-induced hardening; Cycloolefin copolymers

## 1. Introduction

Cycloolefin copolymers (COCs) have received a great deal of attention as photonics materials. There are several types of COCs, but our concern is with the ethylene–norbornene (E–NB) and ethylene–tetracyclododecene (E–TD) copolymers which have enough potential to replace the conventionally used engineering plastics, e.g. polycarbonate, in optical media application because of their high transmissivity, amorphous state, high glass transition temperature $T_g$ and low birefringence. Another advantage lies in their wide range $T_g$ from 0 to 220°C by just varying the comonomer (NB or TD) content. COCs are, therefore, recently being considered for commercial applications [1–3].

Synthetic as well as structural aspect of NB copolymer [4–7] with ethylene and NB homopolymer [8] itself have well been reported, but the processing details are yet to be studied. Eventually, there is no report so far for the highest cyclic olefin, TD content copolymer, except the recent communication of the authors [9]. So, it is worthwhile to study with those copolymers which have immense application in broad range of fields, e.g. optical applications to protective coatings in opto-electronic devices. The chemical structures of E–NB and E–TD copolymer have been shown in Scheme 1.

In this paper, we mainly emphasize on the dynamic and uniaxial elongational behavior of E–NB and E–TD copolymers and the unique behavior of stress optical rule (SOR) under elongation. In our previous publication [9], we reported the composition dependency of elongational viscosity, birefringence and therefore, the stress optical coefficient of E–TD copolymers and here, we report the unique temperature dependency of E–TD copolymers and the difference with E–NB copolymers.

## 2. Experimental

### 2.1. Materials

The E–NB and E–TD copolymers of different NB/TD content were supplied by Mitsui Chemical Inc. The E–NB

* Corresponding author. Tel.: +81-52-809-1861; fax: +81-52-809-1864.
*E-mail address:* okamoto@toyota-ti.ac.jp (M. Okamoto).

0032-3861/01/$ - see front matter 
PII: S0032-3861(01)00508-0

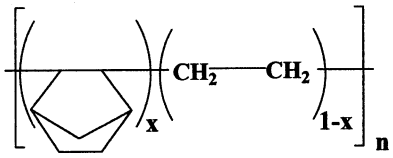


**Ethylene-norbornene (E-NB) copolymer**

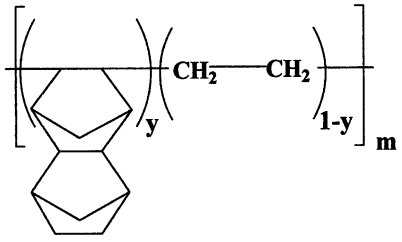


**Ethylene-tetracyclododecene (E-TD) copolymer**

Scheme 1.

copolymers were prepared with different types of metallocene catalyst with wide ranging NB content from 28–60 mol%. According to $^{13}C$ NMR spectra taken by the supplier, the 52 mol% NB copolymer is random copolymer and others are multiblock type possessing small block sequences. On the other hand, the E–TD copolymers were prepared with Ziegler–Natta catalyst and all are random copolymer ranging from 20 to 48 mol% of TD.

The copolymer samples were characterized by using temperature-modulated differential scanning calorimeter (TMDSC, TA2920, TA Instruments) at the heating rate of $5°\,min^{-1}$, to determine $T_g$. The DSC was calibrated with Indium before use. High temperature gel permeation chromatography (GPC: Tosoh HLC-8121 GPC/HT) have been done in *o*-dichlorobenzene carrier at 145.0°C with polystyrene (PS) elution standards. Table 1 summarizes the characteristics of E–NB and E–TD copolymers together with NB/TD content data provided by the supplier.

For comparison, we used linear low density polyethylene (LLDPE; bulk density at 25°C = 0.92 dl/g, weight-average molecular weight $M_w = 4.5 \times 10^5$, the polydispersity index $M_w/M_n = 5.27$ and melting temperature $T_m = 121.9$°C) which was supplied by Asahi Chemical Co.

Table 1
Characteristics of E–NB and E–TD copolymers

| | $DP_w$ [a] | $T_g$ (°C) | $M_w \times 10^{-4}$ | $M_w/M_n$ | Density ($g/cm^3$) |
|---|---|---|---|---|---|
| NB mol% | | | | | |
| 28[b] | 2580 | 76.0 | 12.0 | 2.1 | 1.00 |
| 50[b] | 1480 | 150.0 | 9.0 | 2.4 | 1.02 |
| 52 | 1580 | 132.0 | 9.9 | 2.2 | 1.02 |
| 60[b] | 1640 | 172.0 | 11.1 | 2.8 | 1.02 |
| TD mol% | | | | | |
| 20 | 2300 | 64.0 | 12.5 | 2.7 | 1.02 |
| 23 | 1680 | 80.0 | 9.8 | 3.0 | 1.02 |
| 30 | 1480 | 103.0 | 10.0 | 3.1 | 1.03 |
| 35 | 1480 | 123.0 | 11.0 | 2.8 | 1.04 |
| 41 | 1270 | 146.0 | 10.4 | 2.4 | 1.04 |
| 48 | 1360 | 169.0 | 12.5 | 2.7 | 1.05 |

[a] Degree of polymerization ($DP_w$) $= M_w/[(x_1M_1 + (1 - x_1)M_2]$ where $x_i$ is the mole fraction of the $i$th component in the copolymer and $M_i$ is its molecular weight.

[b] Multiblock type with short block length.

### 2.2. Uniaxial elongation

We carried out the simultaneous measurement of elongational viscosity $\eta_E(\dot{\varepsilon}_0; t)$ and birefringence $\Delta n(\dot{\varepsilon}_0; t)$ at constant strain rate to check the applicability of SOR of various comonomer content of NB and TD in the copolymer on our newly developed *elongational flow opto-rheometry* (EFOR) [10], commercialized Meissner's new elongational rheometer which was coupled with the birefringence apparatus. The details of the instrumentation are describe elsewhere [10,11].

The samples of $60 \times 7 \times 0.5$ $mm^3$ size were annealed at predetermined temperature for 3 min before starting the run in EFOR and uniaxial elongation experiments were carried out at various strain rate $\dot{\varepsilon}_0$ ranging from 1.0 to 0.001 $s^{-1}$.

### 2.3. Dynamic mechanical analysis

Frequency dependence of oscillatory shear moduli in the liquid state was measured, using dynamic frequency sweep tests, on Rheometrics Dynamic Analyzer (RDAII) using parallel plate geometry (25 mm) at various temperatures between $T_g + 30$ to $T_g + 130$°C keeping the strain amplitude of 0.05 to keep linear response of the sample. The measured angular frequency $\omega$ for oscillatory shear experiment is in the range from 0.1 to 100 rad/s. The time–temperature superposition principle was applied to frequency dependence moduli at different temperatures in an attempt to determine the linear viscoelastic properties over a wide range of time scale. The cone-plate geometry (25 mm) was used to measure the zero shear viscosity $\eta_0$ keeping the shear rate $\dot{\gamma}$ of 0.001 $s^{-1}$.

## 3. Results

### 3.1. Glass transition temperature

Fig. 1 shows the variation of glass transition temperature $T_g$ with the comonomer content of NB/TD in E–NB and E–TD copolymers. Here, the $T_g$ of pure homopolymers were taken from the literatures [8,12–14]. The $T_g$ of poly(tetracyclododecene) (PTD) is not reported, but in both copolymer cases, the positive deviation from the additivity rule is clear. Rische et al. [5] showed the linear relation of $T_g$ against NB content of the E–NB copolymers. Probably, they do not take into consideration of the $T_g$ value of pure

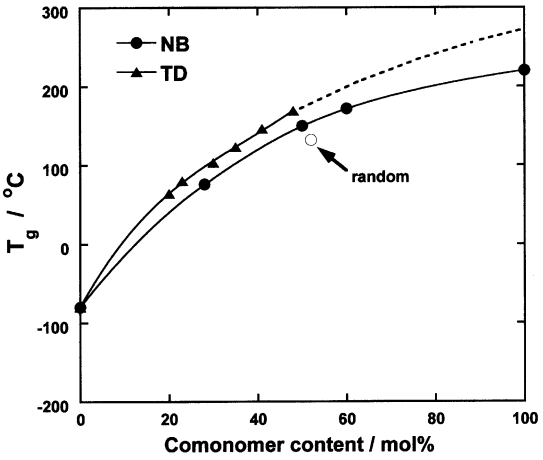


Fig. 1. Dependence of glass transition temperature $T_g$ upon norbornene and tetracyclododecene content (as determined by DSC).

homopolymers, i.e. polyethylene (PE) and poly(norbornene) (PNB). All the E–NB copolymers show only one $T_g$, though they have small multiblock sequences. The copolymer of 50 mol% NB exhibits about 20°C higher $T_g$ compared with random copolymer of 52 mol% NB content.

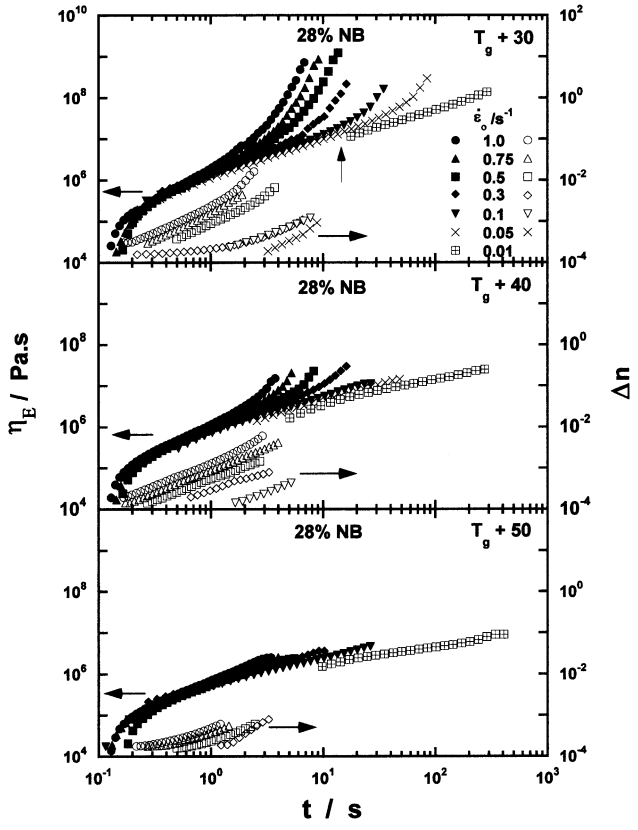


Fig. 2. Double logarithmic plots of transient elongational viscosity $\eta_E(\dot{\varepsilon}_0; t)$ (solid symbol) and birefringence $\Delta n(\dot{\varepsilon}_0; t)$ (open symbol) as a function of time for 28 mol% NB content at indicated temperatures with various Hencky strain rates $\dot{\varepsilon}_0$ as indicated. The upward arrow indicates the uprising time $t_{\eta_E}$ for $\dot{\varepsilon}_0 = 0.1\ s^{-1}$ at which $\eta_E(t)$ begins to deviate from the linear, $\dot{\varepsilon}_0$-independent $\eta_E(t)$ vs. $t$ curve.

In the comparison of TD and NB comonomer species, the $T_g$ of the E–TD copolymers are higher than that of E–NB copolymers over the whole range of composition. This implies that more bulkier TD comonomer than that of NB in the main chain leads to a restricted bond rotation.

### 3.2. Elongational viscosity and birefringence

Fig. 2 shows time variation of $\eta_E(\dot{\varepsilon}_0; t)$ and $\Delta n(\dot{\varepsilon}_0; t)$ of 28 mol% NB copolymer, measured at three different temperatures from $T_g$ + 30 to +50°C. The upward arrow in the figure shows the critical (*uprising*) time $t_{\eta_E}$ at which upward deviation of $\eta_E(\dot{\varepsilon}_0; t)$ from the $\dot{\varepsilon}_0$-independent portion becomes prevailing. We often call the $\dot{\varepsilon}_0$-independent portion, the *linear* portion and the upward deviation, strain-induced hardening [15]. At low temperature elongation ($T_g$ + 30°C), the $\eta_E(\dot{\varepsilon}_0; t)$s show strong strain-induced hardening especially with $\dot{\varepsilon}_0 \geq 0.05\ s^{-1}$, while the strain-induced hardening behavior suppresses drastically with increasing temperatures. At $T_g$ + 50°C, there is no strain-induced hardening observed at any $\dot{\varepsilon}_0$. This behavior seems to be ordinary homopolymer melts [16]. The extent of time

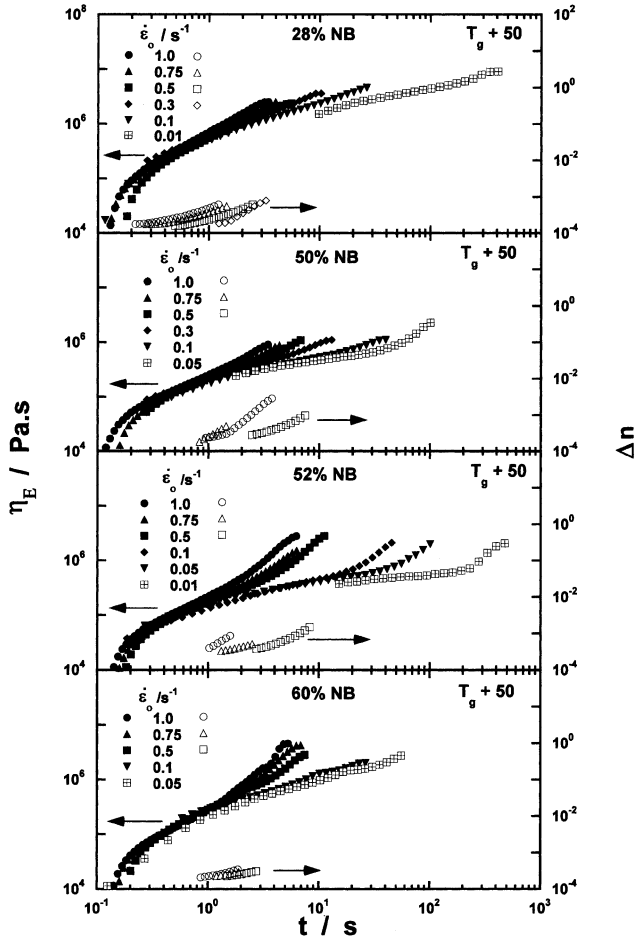


Fig. 3. Double logarithmic plots transient elongational viscosity $\eta_E(\dot{\varepsilon}_0; t)$ (solid symbol) and birefringence $\Delta n(\dot{\varepsilon}_0; t)$ (open symbol) as a function of time with various NB content at $T_g$ + 50°C with various Hencky strain rates $\dot{\varepsilon}_0$ as indicated.

development of $\Delta n(\dot{\varepsilon}_0; t)$ becomes high at low temperature and also gradually decreases with increasing temperatures.

Fig. 3 shows the effect of the comonomer content on the $\eta_E(\dot{\varepsilon}_0; t)$ and $\Delta n(\dot{\varepsilon}_0; t)$ at $T_g + 50$°C. The absolute values of the $\eta_E(\dot{\varepsilon}_0; t)$ of each copolymer are not strongly affected, but the strain-induced hardening behavior emphasizes with increasing NB content. For 52 mol% random copolymer, the strong hardening phenomena is observed compared with 50 mol% copolymer. This is in good agreement with the view that the random copolymer has higher storage $G'(\omega)$ and loss $G''(\omega)$ moduli at low $\omega$ region compared with the copolymer, which has small multiblock sequences, as discuss later in Figs. 7 and 8.

Figs. 4 and 5 show time development of $\eta_E(\dot{\varepsilon}_0; t)$ and $\Delta n(\dot{\varepsilon}_0; t)$ of 30 mol% TD copolymer, measured at three different temperatures from $T_g + 40$ to $+60$°C and the TD content dependence of $\eta_E(\dot{\varepsilon}_0; t)$ and $\Delta n(\dot{\varepsilon}_0; t)$ at $T_g + 50$°C, respectively. At the same temperature range, e.g. $T_g + 50$°C, the TD copolymers exhibit stronger strain-induced hardening than the NB copolymers corresponding to the same ranging in comonomer content. Especially, 48 mol% TD copolymer has anomalous strain-induced

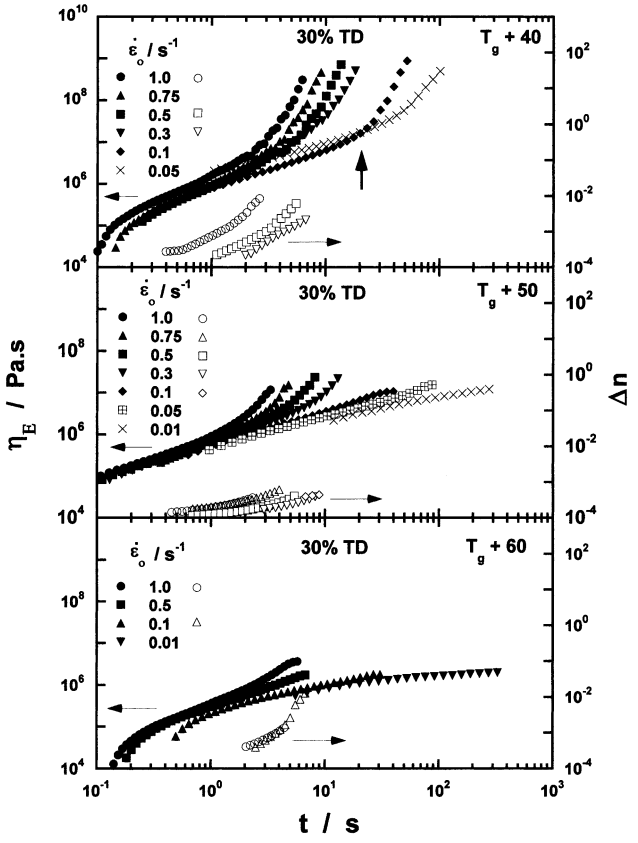


Fig. 4. Double logarithmic plots of transient elongational viscosity $\eta_E(\dot{\varepsilon}_0; t)$ (solid symbol) and birefringence $\Delta n(\dot{\varepsilon}_0; t)$ (open symbol) as a function of time for 30 mol% TD content at indicated temperatures with various Hencky strain rates $\dot{\varepsilon}_0$ as indicated. The upward arrow indicates the uprising time $t_{\eta_E}$ for $\dot{\varepsilon}_0 = 0.1\ s^{-1}$ at which $\eta_E(t)$ begins to deviate from the linear, $\dot{\varepsilon}_0$-independent $\eta_E(t)$ vs. $t$ curve.

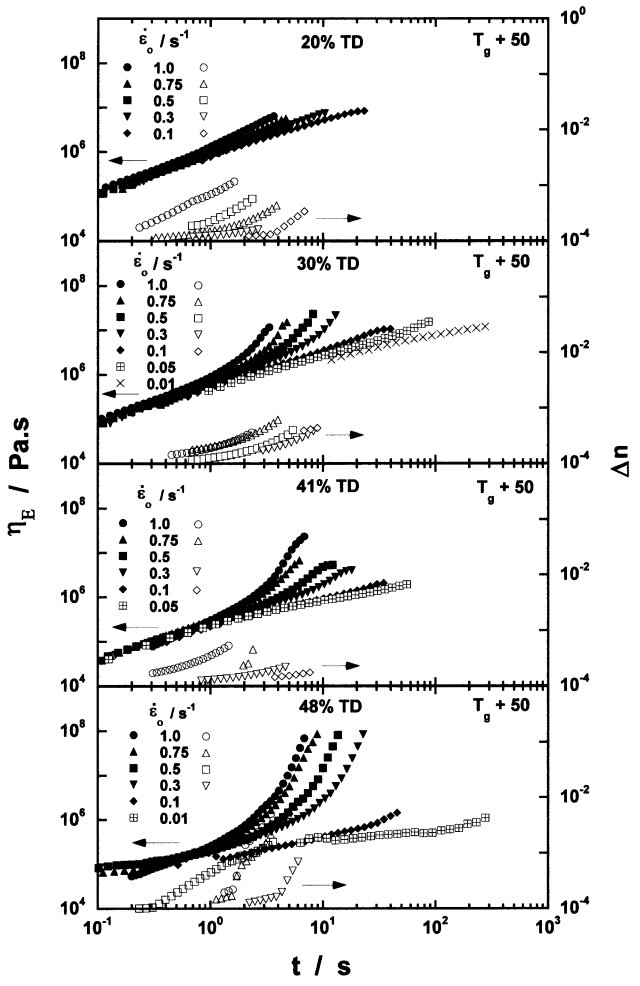


Fig. 5. Double logarithmic plots of transient elongational viscosity $\eta_E(\dot{\varepsilon}_0; t)$ (solid symbol) and birefringence $\Delta n(\dot{\varepsilon}_0; t)$ (open symbol) as a function of time for various TD content at $T_g + 50$°C with various Hencky strain rates $\dot{\varepsilon}_0$ as indicated.

hardening behavior accompanying with increasing of three orders of magnitude of $\eta_E(\dot{\varepsilon}_0; t)$s, although at high temperature elongation ($T_g + 50$°C).

### 3.3. SOR for the E–NB and E–TD copolymers

Fig. 6 shows the stress optical coefficient, $C(\dot{\varepsilon}_0; t)$ ($\equiv \Delta n(\dot{\varepsilon}_0; t)/\sigma(\dot{\varepsilon}_0; t)$ as a function of elongational stress $\sigma(\dot{\varepsilon}_0; t)$ for the eight copolymers obtained at the respective $T_g + 50$°C shown in Figs. 3 and 5. For up to 52 mol% NB copolymers, (Fig. 6(a)) the value of $C(\dot{\varepsilon}_0; t)$ is constant against $\sigma(\dot{\varepsilon}_0; t)$ and all $\dot{\varepsilon}_0$, indicating the SOR is obeyed. However, in the 60% NB copolymer, the downward deviation starts in the early stage of elongation. The excess $\sigma(\dot{\varepsilon}_0; t)$ over developed $\Delta n(\dot{\varepsilon}_0; t)$ might prevail due to the difficulty of both chain alignment and disentangling process for the bulkier and higher comonomer content.

As discussed in our previous paper [9], in the copolymer of 20 mol% TD the SOR roughly holds for every $\dot{\varepsilon}_0$.

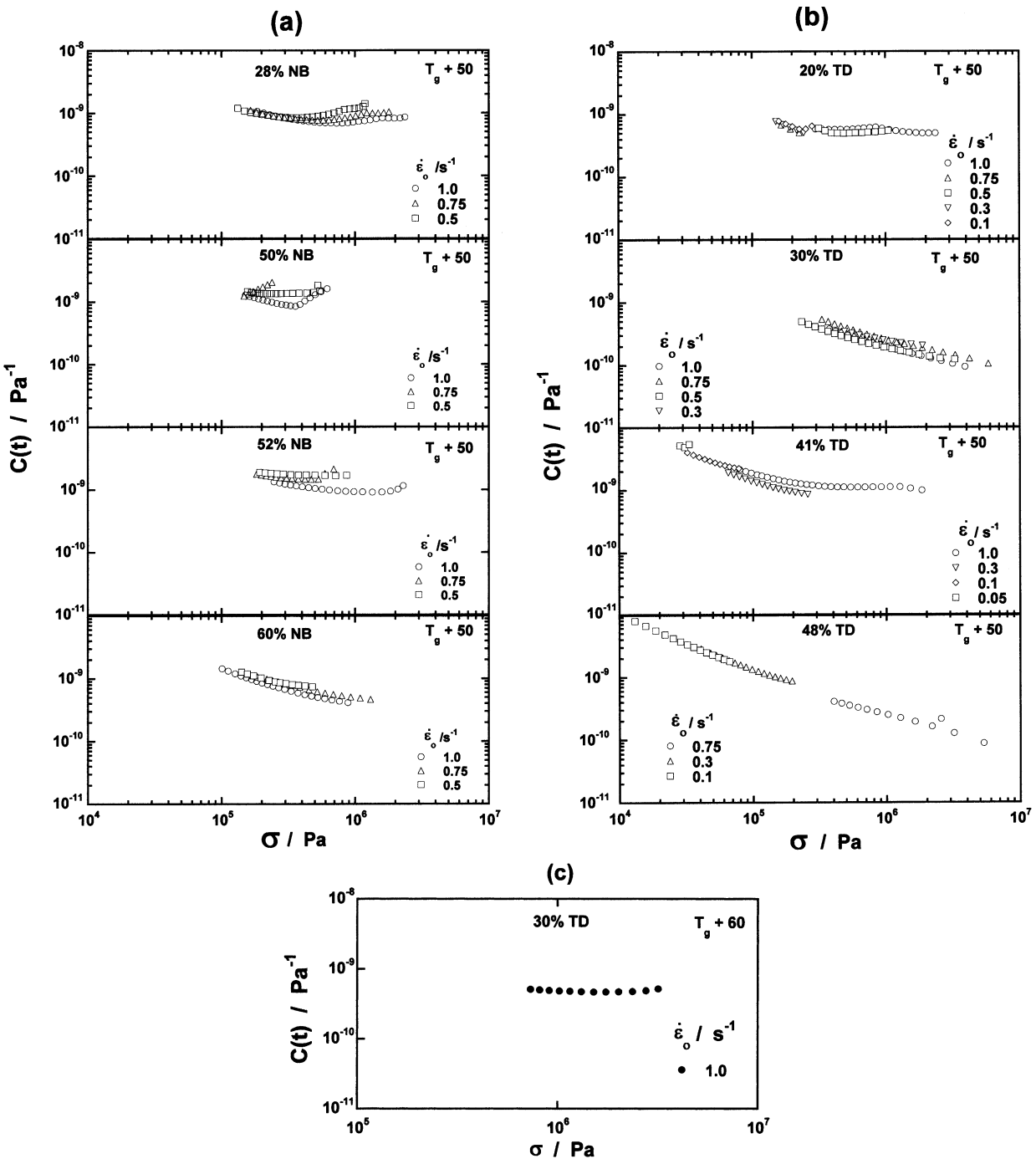


Fig. 6. Stress optical coefficient $C(\dot{\varepsilon}_0;t)$ ($\equiv \Delta n(\dot{\varepsilon}_0;t)/\sigma(\dot{\varepsilon}_0;t)$) of NB and TD content copolymer: (a) E–NB at $T_g$ + 50°C (b) E–TD at $T_g$ + 50°C and (c) 30% E–TD copolymer at $T_g$ + 60°C.

However, for those of higher TD content (≥30 mo% TD) $C(\dot{\varepsilon}_0;t)$ decreases with increasing $\sigma(\dot{\varepsilon}_0;t)$ so that the SOR is invalid as seen in Fig. 6(b). The unique behavior of the SOR is observed in 30 mol% E–TD copolymer. At high temperature ($T_g$ + 60°C) the $C(\dot{\varepsilon}_0;t)$ becomes constant with the whole range of $\sigma(\dot{\varepsilon}_0;t)$ and the strain-induced hardening behavior is not pronounced, like 20 mol% TD copolymer resulted in the validity of the SOR (Fig. 6(c)).

In Table 2, we summarize the validity of the SOR for E–NB and E–TD copolymers. The SOR is valid for E–NB copolymers except 60 mol% NB copolymer at $T \geq T_g + 50$°C and low TD content copolymer (≅20 mol% TD) and is invalid for high TD content (≥30 mol%) copolymer, while there is some temperature dependency of the validity for 30 mol% TD copolymer. In Section 4, we will emphasize on this topic again.

Table 2
Validity of SOR of E–NB and E–TD copolymers ((O) SOR valid; (×) SOR invalid)

| Temperature (°C) | E–NB (mol%) | | | | E–TD (mol%) | | | |
|---|---|---|---|---|---|---|---|---|
| | 28 | 50 | 52 | 60 | 20 | 30 | 41 | 48 |
| $T_g + 30$ | O | O | O | O | – | – | – | – |
| $T_g + 40$ | O | O | O | O | O | × | × | × |
| $T_g + 50$ | O | O | O | × | O | × | × | × |
| $T_g + 60$ | O | | | × | O | O | × | × |
| $T_g + 70$ | O | | | | O | O | O | |
| $T_g + 80$ | O | | | | O | O | O | |

### 3.4. Dynamic moduli and complex viscosity

Fig. 7 shows the comparison of $G'(\omega)$ against reduced angular frequency $a_T\omega$ for E–NB and E–TD copolymers with the reference temperature $T_{ref}$ (= $T_g$ + 50°C). Here, $a_T$ is the WLF-type shift factor determined from dynamic moduli [17]. The insert in each panel is the plot of log $a_T$ vs. $T$–$T_g$. The value of $G'(\omega)$ increases with comonomer content, and this indicated that chain stiffness increases with increasing NB comonomer. In the low-$\omega$ region, the curves can be expressed by a power-law of $G'(\omega) \propto \omega^2$ for 52 mol% random copolymer and $G'(\omega) \propto \omega$ for multiblock type copolymers. The former is similar to those of narrow MW distribution homopolymer melts. On the other hand, the latter resemble block copolymer melts which have the microphase-separated domains [18].

However, E–TD copolymer shows some different behavior. Copolymers containing 20 and 30 mol% TD have the same value of $G'(\omega)$, and it decreases with further increase in comonomer. This decrease in $G'(\omega)$ lies in the fact that degree of polymerization $DP_w$ of E–TD copolymers drastically decreases from 2300 to 1270 for 20 mol% to 41 mol% TD copolymer. Though the chain stiffness increase with the comonomer content, that effect is nullified by $DP_w$ of the copolymer. In this juncture, it is necessary to compare the value of $G'(\omega)$ and $G''(\omega)$ of E–NB and E–TD copolymers with same $DP_w$, even though it is not the absolute value, as measured from GPC, but here, it is enough for comparison purpose.

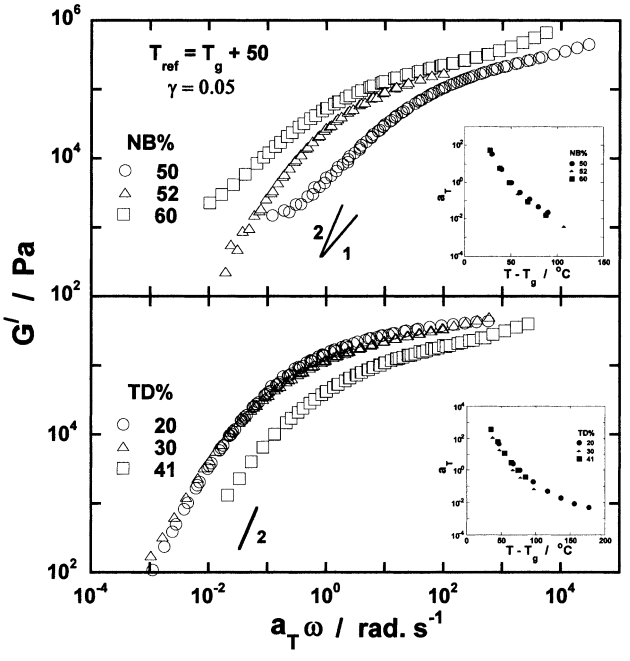


Fig. 7. Plots of storage modulus, G′ vs. reduced frequency, $a_T\omega$ of E–NB and E–TD copolymers with the reference temperature, $T_{ref} = T_g + 50$°C. The shift factors are plotted against $T$–$T_g$ in the inset. The solid lines represent the theoretical slope.

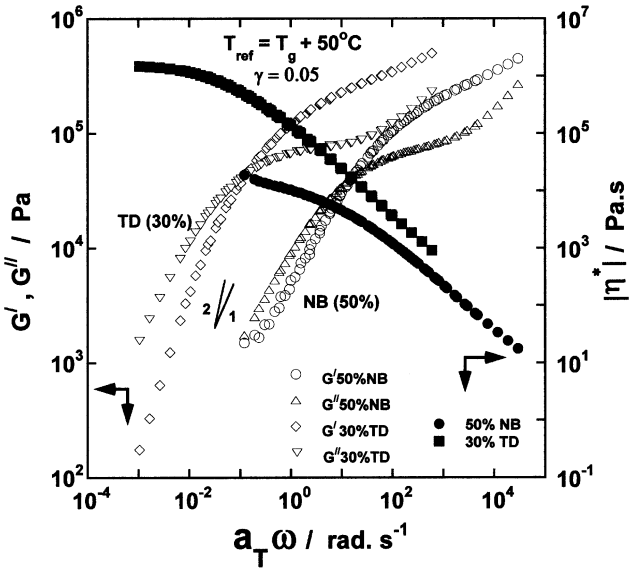


Fig. 8. Reduced frequency dependency of storage, loss modulus and complex viscosities of 50 mol% NB and 30 mol% TD copolymer, having same degree of polymerization ($DP_w$ = 1480). The solid lines represent the theoretical slopes. $T_{ref} = T_g + 50$°C.

Fig. 8 clearly shows that the moduli of 30 mol% TD is much higher than that of 50 mol% NB copolymer, both of which have same $DP_w$ (≅1480). This also supports that chain stiffness increases for E–TD copolymer compared to E–NB copolymer even though the TD content in E–TD copolymer is less. This suggests that the chain stiffness increases with the size of the comonomer. The same thing is also exhibited in higher $T_g$ of E–TD copolymer compared with same NB content in E–NB copolymer as seen in Fig. 1. The complex viscosity $|\eta^*|$, compared at $T_g$ + 50°C, of E–TD copolymer is also higher than that of E–NB copolymer due to the bulkier comonomer of TD. The activation energy for the viscous flow of the COCs was discussed in Appendix A.

## 4. Discussion

### 4.1. $C(\dot{\varepsilon}_0; t)$ vs. comonomer composition

Fig. 9 shows the logarithmic plot of $C(\dot{\varepsilon}_0; t)$ vs. the

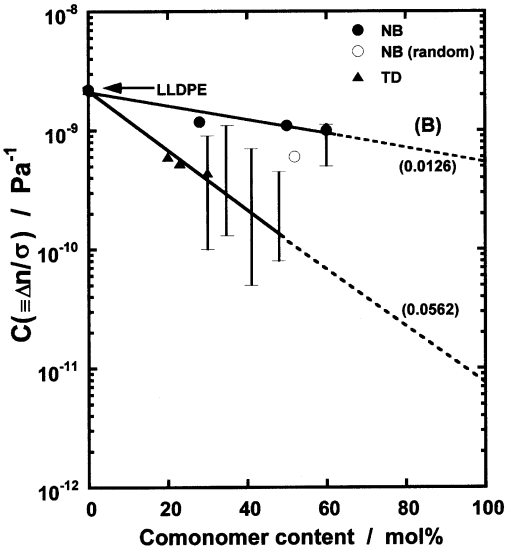


Fig. 9. Stress optical coefficient $C(\dot{\varepsilon}_0;t)$ ($\equiv \Delta n(\dot{\varepsilon}_0;t)/\sigma(\dot{\varepsilon}_0;t)$) as a function of comonomer content (mol%) of E–NB and E–TD copolymer. The numerical values are the calculated slopes of the exponential relation described in text.

amount of comonomer content in the chain. In the figure, the symbols indicate the case of the validity of the SOR, while the ranges show the invalidity of the SOR. In the valid case of the SOR, there is no temperature dependency on the $C(\dot{\varepsilon}_0;t)$ values within the temperature range from $T_g + 30$ to $T_g + 50$°C. Interestingly, the value of $C(\dot{\varepsilon}_0;t)$ is nicely followed by exponential relation given by

$$C(\dot{\varepsilon}_0;t) = k\exp(-Bx) \quad (1)$$

where $k$ is the value of $C(\dot{\varepsilon}_0;t)$ for LLDPE ($\cong 2.2\times 10^{-9}$ Pa$^{-1}$) obtained in this study and $B$ is the slope and $x$ is the comonomer content. The $C(\dot{\varepsilon}_0;t)$ for random E–NB copolymer is lower than that of block type E–NB copolymer and the values of $C(\dot{\varepsilon}_0;t)$ of E–TD copolymer with different compositions are lower than that of E–NB copolymers. Furthermore, the E–TD copolymers have large value of $B$ compared to E–NB copolymers. The $B$ values are 0.0126 and 0.0562 for E–NB (block type) and E–TD copolymer, respectively.

After extrapolation to 100 mol% comonomer content with an assumption of Eq. (1), we can obtain the $C(\dot{\varepsilon}_0;t)$ value of norbornene and tetracyclododecene homopolymer. The $C(\dot{\varepsilon}_0;t)$ of PNB (block type) and PTD are $5.5\times 10^{-10}$ and $7.5\times 10^{-12}$ Pa$^{-1}$, respectively. The PNB has the same order of $C(\dot{\varepsilon}_0;t)$ for poly(methyl methacrylate) (PMMA) ($\cong -2.0\times 10^{-10}$ Pa$^{-1}$), which is reported in our previous paper [19]. For the PTD, the magnitude of $C(\dot{\varepsilon}_0;t)$ is two order lower than PMMA.

### 4.2. Elongational flow-induced strain hardening

The decreasing tendency of strain-induced hardening for E–NB and lower TD content of E–TD copolymer with increasing temperatures is not surprising. With the increase in temperature, the melt viscosity decreases and accordingly, the hardening phenomena gradually abolish. In the case of E–NB copolymer, SOR is almost valid, and it is more resemble like LLDPE, for all comonomer compositions, $\dot{\varepsilon}_0$s and temperatures measured. The only thing is that with extent of comonomer content the strain-induced hardening behavior increase for E–NB copolymer. Complicity arises from 30 mol% TD of E–TD copolymer, for which SOR is invalid at low temperature, but valid at high temperature ($= T_g + 60$°C), where strain-induced hardening is its minimal (cf. Table 2). At high temperatures, due to the low melt viscosity, the polymer chains can align nicely in the direction of stretching as a result $\Delta n(\dot{\varepsilon}_0;t)$ as well as $\sigma(\dot{\varepsilon}_0;t)$ increase with time and/or strain, thereby the SOR become valid. This alignment of chain is difficult at low temperatures ($= T_g + 40$°C), so $\Delta n(\dot{\varepsilon}_0;t)$ is not increasing so much, while $\sigma(\dot{\varepsilon}_0;t)$ increases with time gradually causing the value of $C(\dot{\varepsilon}_0;t)$ to decline with increasing $\sigma(\dot{\varepsilon}_0;t)$. With the further increase in TD comonomer ($\geq$41 mol% TD) strain-induced hardening phenomena observed for all $\dot{\varepsilon}_0$s and temperatures measured. The population of bulkier comonomer is such that even at high temperatures, ($= T_g + 60$°C), low melt viscosity, it is difficult to stretch the polymer chain exhibiting strong strain-induced hardening as a result the SOR become invalid for the whole range of temperature.

### 4.3. Uprising Hencky strain

As seen in Figs. 2–5, the $\eta_E(\dot{\varepsilon}_0;t)$s increase rather rapidly at the $t_{\eta_E}$, marked with the upward arrows. On elongation of homopolymer melts, the upward deviation of $\eta_E(\dot{\varepsilon}_0;t)$ by the strain-induced hardening takes place at a common *uprising* Hencky strain $\varepsilon_{\eta_E}$ ($= \dot{\varepsilon}_0 t_{\eta_E} \approx$ constant) which is insensitive to the either strain rate $\dot{\varepsilon}_0$ or temperature of elongation [20].

In Fig. 10, we plotted $\varepsilon_{\eta_E}$ of E–NB and E–TD copolymers as a function of comonomer content. Inset figure represents $\varepsilon_{\eta_E}$ of LLDPE at various temperatures which show constancy with the temperatures measured. The E–NB copolymer exhibit almost constant $\varepsilon_{\eta_E}$ ($\sim$1.2–1.3) with the comonomer content, but the average value is slightly higher than the measured value of LLDPE ($\varepsilon_{\eta_E} \sim 1.2$), indicated with the dotted line. For the E–TD copolymers, the $\varepsilon_{\eta_E}$ increases with the comonomer contents for all the temperatures and, for a particular copolymer composition, the $\varepsilon_{\eta_E}$ decreases with increasing temperatures. Before the alignment of polymer chain under uniaxial elongation, one has to consider the disentangling process first, and then, the chain molecule can orient itself in the stretching direction. At high temperature, low melt viscosity, the disentangling process is favored, and as a result, the polymer chain face the hindrance from its bulkier comonomer at the early stage giving rise to low $\varepsilon_{\eta_E}$. With the increase in comonomer population (high comonomer content copolymer), the

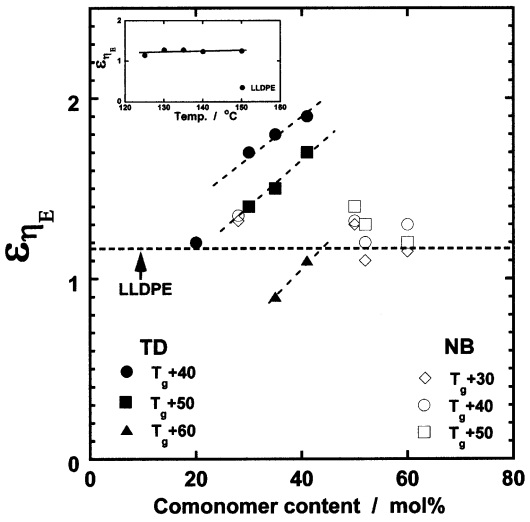


Fig. 10. Plots of uprising Hencky strain ($\varepsilon_{\eta_E} = \dot{\varepsilon}_0 t_{\eta_E}$) vs. commoner content at indicated temperatures for E–NB and E–TD copolymers. The uprising time, $t_{\eta_E}$ is shown by arrow in Figs. 2 and 4. The dotted line represents the $t_{\eta_E}$ for LLDPE and the insert shows the experimental data for LLDPE.

disentangling process is presumably disfavored, uncoiling of chains take place at longer time and/or larger strain, give rise to high $\varepsilon_{\eta_E}$. The same reason also may be applicable to E–NB copolymers where $\varepsilon_{\eta_E}$ is higher than the LLDPE and somehow E–NB copolymers resemble more like LLDPE and show constant $\varepsilon_{\eta_E}$.

## 5. Conclusion

Both the glass transition temperature and modulus increase for E–TD copolymer compared to E–NB copolymer, indicating the increase in chain stiffness with the bulkier comonomer. COCs with its bulkier comonomer show strong strain-induced hardening behavior, and the SOR is almost obeyed for the whole range of composition for E–NB and low comonomer content E–TD copolymer (<30 mol% TD), but SOR is invalid for high TD content copolymer (≥30 mol%). The $C(\dot{\varepsilon}_0; t)$ decrease exponentially with the comonomer content, and the decreasing rate is governed by the comonomer size. The $C(\dot{\varepsilon}_0; t)$s, calculated from the extrapolation curve of E–NB (block type) and E–TD copolymer at zero E limit, were expected to be $5.5 \times 10^{-10}$ and $7.5 \times 10^{-12}$ $Pa^{-1}$, respectively. The $\varepsilon_{\eta_E}$ is closely related to the disentangling process, which is governed by the size of the comonomer species and its content.

## Acknowledgements

We wish to thank Mitsui Chemical Inc. for providing COC samples with different compositions.

## Appendix A. Flow activation energy and free volume fraction

Fig. 11 shows the typical result of the zero shear viscosity $\eta_0$ (fitted with Ellis model) of COCs vs. reciprocal temperature $1/T$ at temperature from $T_g + 30$ to $+100$°C. For the E–NB and E–TD copolymers, the plots nicely conform to straight lines, as predicted by an Arrhenius-type equation given as

$$\eta_0 \sim \exp(E_a/RT) \tag{A1}$$

where $E_a$ is the apparent activation energy for the viscous flow and $R$ is the gas constant. The obtained value of $E_a$ for each copolymers are replotted against comonomer content as shown in Fig. 12. For comparison, the $E_a$ of the LLDPE is measured similarly. The COCs have much higher value of $E_a$ than that of the LLDPE. It reveals that after certain mol% of comonomer (>40 mol%) of E–NB copolymer, the value of $E_a$ is leveling off, while for E–TD copolymer, it increases continuously. From this fact, one gets the idea why it is so

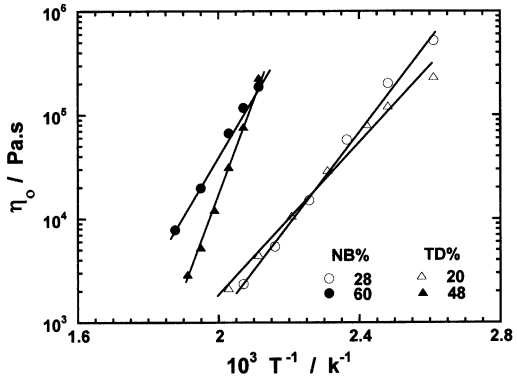


Fig. 11. Plots of zero shear viscosity, $\eta_0$ vs. inverse temperature at indicated two different comonomer composition for E–NB and E–TD copolymers. From the slope of the straight line the flow activation energy, $E_a$ was calculated.

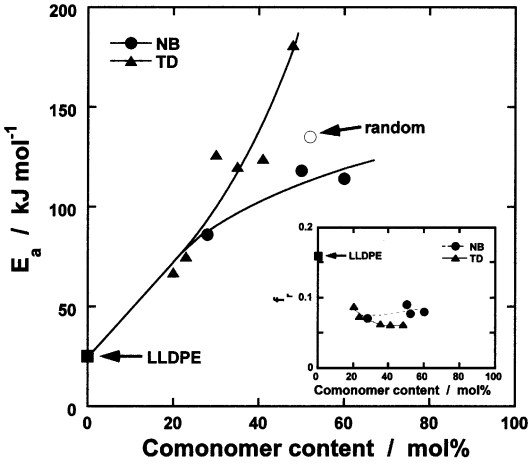


Fig. 12. Flow activation energy, $E_a$ vs. comonomer content (mol%) for E–NB and E–TD copolymer. The inset shows the free volume fraction, $f_r$ of E–NB and E–TD copolymer. Both the results are compared with LLDPE.

difficult to prepare the PTD homopolymer when PNB can be prepared after taking some measure. Flow activation energy of E–TD copolymer is so high that the diffusion of growing polymer chain during polymerization is very difficult. Haselwander et al. [8] reported the PNB of moderately high molecular weight. They also reported the dense packing of the PNB in the amorphous state, which is also reflected in our low free volume fraction of COCs compared to the linear polyethylene. The inset of Fig. 12 shows the free volume fractions $f_r$ calculated by

$$f_r = \frac{1}{2.303 c_1} \tag{A2}$$

where $c_1$ is the constant of WLF-type equation. The $f_r$s of NB and TD copolymers decrease significantly compared to the LLDPE. This indicates that the close packing in the amorphous state occur as revealed by higher density with increasing comonomer contents (cf. Table 1).

## References

[1] Tokkyo-kouhou H4-48803; H4-48803, Mitsui Petrochemical Co., Inc.
[2] Hoechst AG. Hoechst Mag Future 1995;IV:52.
[3] Hoechst AG. Hoechst Mag Future, Spec Sci 1 1995;IV:32.
[4] Kaminsky W, Bark A, Arndt M. Makromol Chem Macromol Symp 1991;47:83.
[5] Rische T, Waddon AJ, Dickinson LC, MacKnight WJ. Macromolecules 1998;31:1871.
[6] Chu PP, Huang WJ, Chang FC, Fan SY. Polymer 2000;41:401.
[7] Cherdron H, Brekner MJ, Osan F. Die Angew Makromol Chem 1994;223:121.
[8] Haselwander FAT, Heitz W, Krugel SA, Wendorf JH. Macromol Chem Phys 1996;197:3435.
[9] Maiti P, Okamoto M, Kotaka T. Polymer 2001;42:3939.
[10] Kotaka T, Kojima A, Okamoto M. Rheol Acta 1997;36:646.
[11] Meissner J, Hostettler J. Rheol Acta 1994;33:1.
[12] Illers KH. Kolloid-Z Z Polym 1969;231:622.
[13] Illers KH. Kolloid-Z Z Polym 1974;251:1.
[14] Illers KH. Kolloid-Z Z Polym 1973;151:394.
[15] Larson RG. J Rheol 1984;28:545.
[16] Janeschitz-Kriegel H. Polymer melt rheology and flow birefringence. New York: Springer, 1983.
[17] Williams ML, Landel RF, Ferry JD. J Am Chem Soc 1955;77:3701.
[18] Bates FS. Macromolecules 1984;17:2607.
[19] Knao Y, Okamoto M, Kotaka T. Polymer 1999;40:2459.
[20] Schlund B, Utracki LA. Polym Engng Sci 1987;27:359.